16th World Conference on Earthquake, 16WCEE 2017

Santiago Chile, January 9th to 13th 2017

Paper N° 4671

Registration Code: S-I1464746868

STRONG-MOTION GENERATION AREAS OF THE 2007 Mw8.0 PISCO, PERU, EARTHQUAKE USING THE EMPIRICAL GREEN'S FUNCTION

N. Macavilca-Rojas[(1)], T. Yokoi[(2)], T. Hayashida [(3)]

[(1)] *Research Assistant, CISMID, Faculty of Civil Engineering, National University of Engineering, Lima, Peru*
nadia.macavilca.r@uni.edu.pe
[(2)] *Director, International Institute of Seismology and Earthquake Engineering*
Building Research Institute, Japan, tyokoi@kenken.go.jp
[(2)] *Senior Research Scientist, International Institute of Seismology and Earthquake Engineering*
Building Research Institute, Japan, takumi-h@kenken.go.jp

Abstract

The size of the strong motion generation areas (SMGA) and rise time for the Mw8.0 August 15, 2007 Pisco, Peru Earthquake were determined using the Empirical Green's function method (EGFM) to synthetize waveforms in the frequency range between 0.1 and 1 Hz at seismic stations MOL and PRC. The criteria of Somerville et al. (1999) was applied to the slip distribution rupture model (Sladen et al, 2010) obtaining a two asperities source model as initial approach of the SMGAs. The observed waveforms of the mainshock were also divided in two wave packets to compute the contribution from each SMGA independently, by using two aftershocks (*Mw*5.6 and *Mw*5.0) as Empirical Green's functions (EGF). The spectral analysis of the waveforms did not follow the omega-squared source spectra model, therefore the SMGAs (SMGA1 and SMGA2) were obtained by a grid searching, considering correlation coefficients and visual comparisons between the successive observed and synthetic waveforms. The agreement between the observed and synthesized waveforms from SMGA2 were poor, compared with those for SMGA1, moreover the source area parameters and amount of average slips for asperities followed the scaling laws for interplate earthquakes.

Keywords: EGFM; SMGA; Pisco Earthquake.

1. Introduction

The 2007 Mw8.0 Pisco earthquake (15 August, 2007) produced strong ground shaking through the central coast of Peru, causing extensive damage to non-engineered dwellings, interruption of the Pan-American South Highway and ground failure by liquefaction. Following the disaster, regional seismicity, dynamic characterization of soils, site effect and seismic microzonation studies have been conducted in order to assess the seismic hazard. The 2007 Pisco earthquake was a megathrust event that occurred along the interface of the Nazca and South American plates with a recurrence interval of 250 years (Perfettini et al., 2010). The estimated source rupture models indicate the complexity of its source rupture process. The teleseismic inversion suggests that the earthquake is composed of two subevents (e.g. Sladen et al., 2010), while back projection images show three energy peaks (Lay et al., 2010). Possible megathrust earthquake scenarios (Mw 8.9) based on an interseismic coupling model, scenario geodetic measurements, and historical seismicity were proposed by Pulido et al. (2013). Therefore, the synthetizing of strong ground motions of Pisco earthquake are important to evaluate the ground motion intensity in different sites and accordingly take policies of disaster prevention. The purpose of this study is to model the SMGA of the 2007 Pisco earthquake using the Empirical Green's Function Method proposed by Irikura (1986) and validate the obtained source parameters with the scaling laws for major interplate earthquakes.

2. Empirical Green's Function Method

In this study the empirical Green's function method (EGFM) proposed by Irikura (1986) is used. This method is based on the self-similar scaling laws of fault parameters between large and small earthquakes (Kanamori and Anderson, 1975) and the omega-squared (ω^2) source spectral model (Aki, 1967; Brune, 1970; 1971).

This method synthetize strong-motion time histories of a large earthquake using waveforms of small earthquakes as empirical Green's function (EGF). The EGF contains actual information of the initial rupture process, effects of propagation path between the source and site and site amplification at seismic observation station. Synthetic waveform of the target event $U(t)$ is obtained by summing up the element event waveform $u(t)$ convolved by a filter function $F(t)$ as shown in Eq. (1), using scaling factors of fault dimension N and stress drop C between small and large earthquakes (Figure 1). The delta and exponentially- decaying functions $F(t)$ (Eq. (2)) proposed by Irikura et al. (1997) corrects the velocity time function between the target and element earthquakes and t_{ij} (Eq. (3)) is the time difference between the starting rupture point and the ij-th location of the subfault.

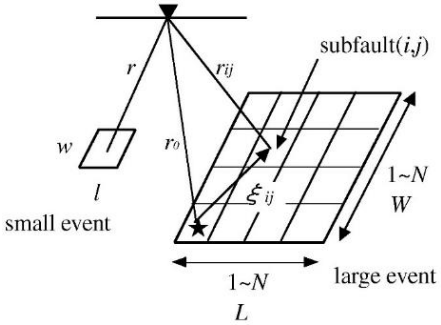

Fig. 1 – Spatial schema of parameters and variables used by the Empirical Green's Function Method, Source: IISEE Lecture Note 2014-2015.

$$U(t) = \sum_{i=1}^{N}\sum_{j=1}^{N} \frac{r}{r_{ij}} F(t) * \ (C \cdot \ u(t)) \tag{1}$$

$$F(t) = \delta(t - t_{ij}) + \frac{1}{n'(1-\frac{1}{e})} \sum_{k=1}^{(N-1)n'} [\frac{1}{e^{\frac{(k-1)}{(N-1)n'}}} \delta\{t - t_{ij} - \frac{(k-1)T}{(N-1)n'}\}] \tag{2}$$

$$t_{ij} = \frac{r_{ij} - r_o}{V_s} + \frac{\xi_{ij}}{V_r} \tag{3}$$

The source spectrum of large earthquakes with complex rupture process such as the Pisco earthquake does not follow the ω^2 model, and therefore the source model should be characterized by asperity models. The asperities, the large slip areas during the mainshock, are considered as the 'locked' areas over the entire source fault and can be used as the initial SMGAs, which in turn are the areas with a large uniform slip velocity or high stress drop in all the rupture area (Miyake et al., 2003). The criterion of Somerville et al. (1999) can be used to identify the asperities from the existing finite-fault models. Finally the SMGAs are determined by successive comparison of observed strong motion waveforms of the target earthquake with the synthetics calculated by the EGFM.

3. Source model of the 2007 Mw8.0 Pisco, Peru Earthquake

3.1 Source model of the 2007 Mw8.0 Pisco, Peru Earthquake

The source slip distribution model with variable slip rise time and rupture propagation by Sladen et al. (2010) was used to identify the asperities of the 2007 Pisco earthquake (Figure 2). By the application of the criteria of Somerville et al. (1999), the reduced source model (thick blue line in Fig. 2) with rectangular asperities; ASP1 (36 kmx30 km) and ASP2 (60 kmx60 km) were identified (thick red rectangles in Fig. 2). The hypocenter is located on the asperity ASP1. The rupture front propagation is the same as that of Sladen et al. (2010).

Table 1 – Characteristics of the variable slip distribution model of the Pisco Earthquake 2007 (23:40:57 UTC) and isometric view scheme of the "s2007PISCOP01SLAD". Source: e-Quake RC.

Seismic moment	(Nm)	1.12E+21
Strike	(°)	318
Average Dip	(°)	20.95
Rake	(°)	59.46
Length	(km)	576
Width	(km)	210
Htop	(km)	2.39

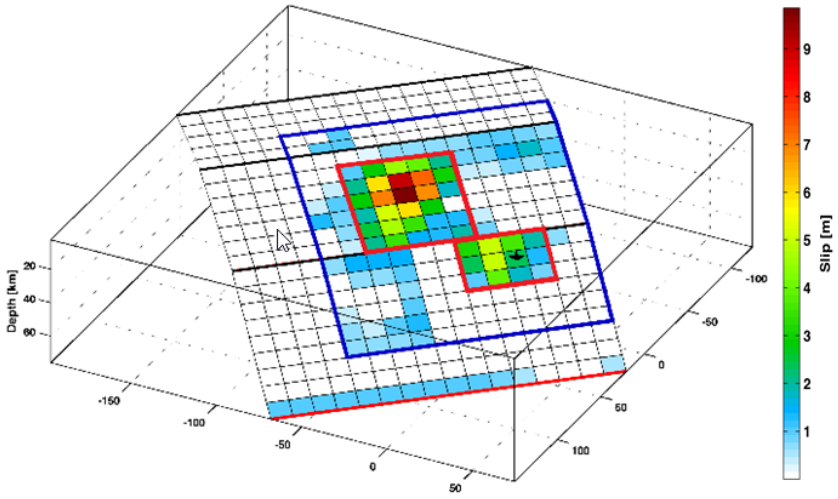

Fig. 2 – Characteristics of the variable slip distribution model of the Pisco Earthquake 2007 (23:40:57 UTC) and isometric view scheme of the "s2007PISCOP01SLAD". Source: e-Quake RC. The thick blue line marks the reduced fault model and the thick red line the asperities.

3.2 Strong-motion data

The mainshock and aftershock records at stations Molina (MOL) at Lima Metropolitan City and Parcona (PCN) at Ica Department were analyzed. PCN was the only station located as an extension of the rupture propagation direction, and MOL was chosen from all the stations in Lima City because of negligible amplification effects in the frequency range of study (Quispe et al., 2013). Two aftershock recording were selected as EGFs considering the available records and their hypocentral locations (Table 2 and Figure 3). Before the computation, the mainshock signals were divided in two portions corresponding to the first (SMGA1) and second events (SMGA2), choosing the split points between the two peaks from the minimum amplitude portion. It was not possible to obtain the scaling factors N and C using the source spectral ratio fitting method, because the acceleration spectra of the subevents MOL and PCN does not follow the omega-square pattern. It was also impossible to increase the signal-to-noise ratio by averaging the SSRF of many stations due to the lack of data. Finally, the analysis and SMGA identification was done for the grid searching.

Table 2 – Hypocentral characteristics of the two events used as Green's Functions.

Event	**Aftershock 1 (EGF 1)**	**Aftershock 2 (EGF 2)**
Magnitude	5.6 m_b	5.0 Mw
Seismic Moment (N.m)	2.82E+17	4.38E+16
Date and Hour GMT+0	2007.08.16 00:02:41	2010.11.03 10:45:22
Latitude (°)	-13.255	-13.699
Longitude (°)	-76.489	-76.097
Depth (km)	39.6	37.9
Strike φ / Dip δ / Rake λ (°)	318/21.0/59.5	314/44/40

4. Results

4.1 Strong Motion Generation Areas

The original three-segmentation fault model with variable dip angle (δ =6º, 20° and 30°) were projected to a plain containing dip angle of the middle segment (δ =20º). The hypocenter depth of the mainshock on the SMGA1 was shifted to the source of the new source model. The effect of this one-dip source model does not much affect the travel time of seismic signals, thus it was neglected. The frequency range for the simulation was between 0.1 and 1 Hz. The first approach for synthesize the strong motion records was to scale the rupture area of the element earthquake to the area of the initial SMGA (ASP) trying with different values of N and choosing the initial rupture point by the original front rupture (Sladen et al., 2010). By the grid searching, the values for factors N, dimensions of the element earthquake (l and w), rupture velocity (Vr), S-wave velocity (Vs) and rise time (τ) were estimated.

The SMGA model that generates the smaller residual factor and best correlation factor (closest to one) between the observed and synthetic strong motion record was the selected model for each SMGA. The factors C were tuned to match the peak amplitudes of the time histories and in some cases its value was increased in order to compensate the lack of frequencies.

During the grid searching, and following the mentioned criteria, it was noticed that the model that generates the best synthetic waveform to MOL station signal was not the appropriate to simulate PCN signal and vice versa in both SMGAs. As shows Table 3, it was necessary more quantity of EGFs (N) to generate the PCN signal in comparison to the case of the further station, MOL. Also, the rising time for the simulation of PCN signal was bigger than the rising time fitting the MOL signal. Despite the difference between the models, the areas, its rupture velocity and S-wave velocity values are close.

Table 3 – Source parameters of strong motion generation area.

	Model	**N**	**C**	**L (km)**	**W (km)**	**S (km^2)**	**V_r (km/s)**	**V_S (km/s)**	**T (s)**	**Stations**
SMGA 1	1	2	1 / 3.5	22.0	30.0	660	2.4	3.34	1.0	MOL
	2	3	4.5	22.5	31.5	709	2.4	3.34	1.5	PCN
SMGA 2	1	5	7.0	65.0	45.0	2925	2.6	3.61	1.5	MOL
	2	6	1.1	66.0	42.0	2772	2.4	3.34	1.8	PCN

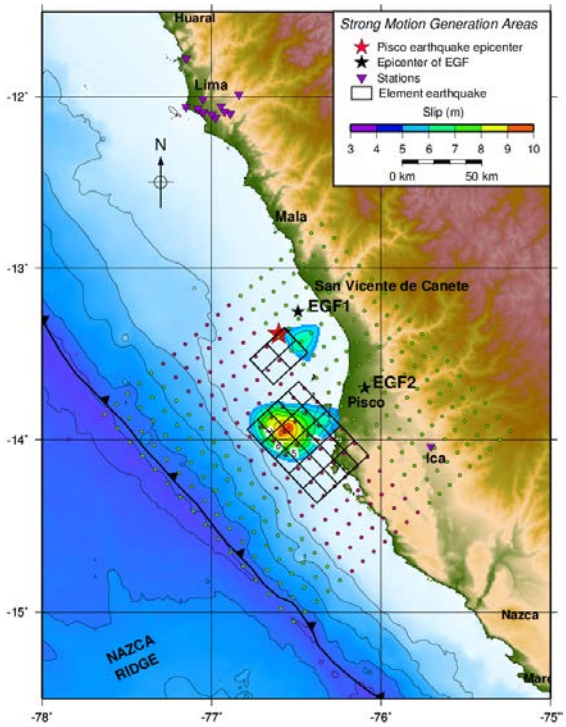

Fig. 3 – Location of the Strong Motion Generation Areas (SMGA) and Sladen et al. (2013) slip distribution. GEBCO Grid (http://www.gebco.net).

In general, the final values of N for the SMGA were inversely proportional to the magnitude of the EGF. The estimated rise times T for both models, were 1.3 s for the SMGA1 and 1.0 s for SMGA2. The area of the element earthquake between SMGA1 and SMGA2 was almost constant, but the w-l ratio was inverted. The similarity between the EGFs area was expected because their similar magnitudes. The sizes and locations of the SMGAs are different from the asperities. The area of the SMGA1 is approximately 64% of ASP1, and the area of the SMGA2 is approximately the 80% of ASP2. The combined area of the ASPs is 4680 km2 and that of SMGAs is 3533 km2. The source parameters of the SMGAs and its models to each station are listed in Table 3. Figure 3 shows the point sources of the original source model and slip values (Sladen et al., 2010) and the SMGA location (rectangular mesh).

4.2 Synthetic waveforms

All the signals were band-pass filtered in the frequency range between 0.1 to 1 Hz before the computation. In the case of station PCN, there was also necessary to be resampled at 20 Hz. Figure 4 shows an example of the comparisons of observed and synthetic waveforms with the EGFM. The envelopes of the synthetic displacement and velocity waveforms have a good correspondence with the observed ones. However, peak amplitudes of accelerograms are underestimated. In general, envelope of the both the synthetic and observed waveforms match better for the SMGA1 than for the SMGA2 and the frequencies larger than 0.5 Hz were attenuated. The main discordance is observed during the first 20 seconds of the SMGA2 waveforms.

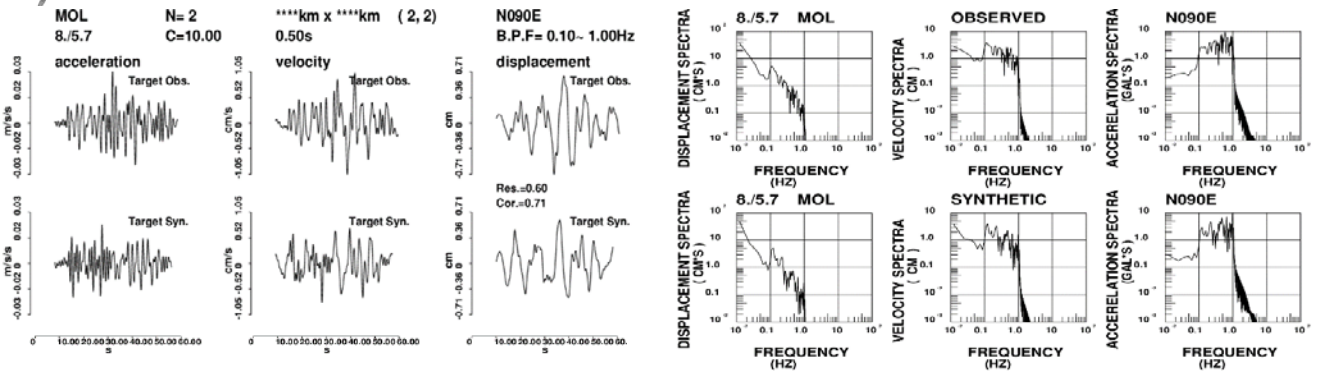

Fig. 4 – Observed and synthetic time history and spectrum of the SMGA1 (station MOL).

5. Discussion

The source model of the 2007 Pisco, earthquake has two-rupture process with a velocity rupture of 2.4 km/s2 and two regions concentrating larger slip, asperities, and included a delay time of 38 seconds between the rupture starting times of both subevents to explain the arrival time delay (Sladen et al., 2010). Nevertheless, back projection analysis identifies three energy sources (IRIS, 2007) as well as the IGP identify three clusters of aftershock spatial distribution. This feature shows the complexity of the rupture process in time and space. In this study the earthquake mainshock data were divided in two wave packs, corresponding to two SGMAs based on two asperities. Followingly, the analysis for each SMGA was made independently without taking the velocity rupture variation and the 38 seconds delay in account to explain rupture process. As the individual wave packets of the mainshock and aftershock waveforms did not follow the ω2 model, the locations of SMGAs were identified by the grid searching. The rupture starting point was selected according to the rupture front obtained by Sladen et al. (2010) and the similitude between the envelopes of the synthetic time history and the observed waveforms. The coefficients between the observed and synthetics waveforms were small, even good similarities were visually observed for waveforms and Fourier spectra. Therefore another more appropriate measure of similarity of waveforms is needed.

The area of the SMGAs is smaller than those of the ASPs and their locations were also different. In general the waveform similarity for the SMGA2 was not as good as the simulation of the SMGA1. This may be due to the interference of the energy released by the first SMGA1. Possible causes of incertitude were the lack of waveforms data and poor station distribution, which made difficult to tune the identification of SMGAs. Another possibility is that, as the back projection and spatial distribution of aftershocks suggest, the SMGA2 possibly corresponds to two smaller SMGAs. Nevertheless the criteria to identify asperities of Somerville et al. (1999) do not let to divide SMGA2 in two SMGAs. Hence, it is necessary to innovate another method to identify SMGAs very close to each other. It was not possible to verify that the EGFM cannot reproduce the frequency equivalent to the inverse of the rise time (Valenzuela Bize, 1997) because the inverse of the rise time of the EGF (0.3 s and 0.5 s) is out of the frequency range for the analysis.

The source model characteristic (Table 2) was compared with the scaling properties of characterized slip models for plate-boundary earthquakes of Murotani et al., (2008). The ratio of the combined area of SMGAs and ASPs is approximately 0.76, which is different from the ratio obtained empirically for the Japanese interplate earthquakes of 0.35 (Tajima et al., 2013).

6. Conclusions

The slip distribution model obtained by inversion (Sladen et al., 2010) identify two patches with concentration of larger slip values, named asperities, which are considered a good approximation to SMGA. On the other hand, back projection analysis find three beam power sources that have been associated with SMGA in previous studies. However, the source model of the Mw8.0 2007 Pisco, Peru earthquake does not follow the omega-

square source spectra model due to its complicated source process. Therefore it is not possible to apply the Source Spectra Ratio Fitting and neither to obtain the values of N and C.

Applying the criteria of Somerville et al. (1999), we obtained SMGA1 and SMGA2 from the two asperities, where each SMGA corresponds to a subevent. The final location and size of the SMGA where obtained by grid search. The SMGA1 and SMGA2 have rupture velocities of 2.4 km/s2 and 2.6 km/s2 respectively with average rise time of 1.5 s (Table 5). The dimension of the SMGA is smaller than those of the ASP, and they are also lightly shifted in comparison to the ASP. The area of the SMGA1 is approximately 64% of the ASP1 area, and the area of the SMGA2 is approximately the 80% of ASP2.

Different rupture starting points into the SMGA2 gave acceptable synthetic waveform, therefore the rupture starting point was chosen in function of the closeness to the rupture front obtained by Sladen et al. (2010).

The 2007 Pisco, Peru Earthquake whole synthetic waveforms of stations PCN and MOL were obtained joining the waveform obtained by grid searching of each SMGA without taking in account the 38 seconds delay imposed by Sladen et al. (2010) to explain the rupture process. The synthetic waveforms matched properly the observed ones, despite the low correlation factors obtained to the waveforms of SMGA2. The waveforms obtained from the SMGA2 show less visual similitude between observed and synthetized waveforms, and also show the lowest correlation factor (0.17 to PCN). It is possibly due to the interference of the rupture process of the SMGA1 and also that the SMGA2 may correspond to two smaller and close SMGAs.

Our results indicate the necessity of further research to characterize the SMGA of the 2007 Pisco, Peru Earthquake, and test it with another records, taking in account the possibility of divide the SMGA2 in two smaller SMGAs, as the back projection analysis suggests.

The source and asperities areas, and average slips for asperities follow the scaling laws for interplate earthquakes for plate-boundary earthquakes (Murotani et al., 2008) but the ratio of SMGAs and ASPs areas of 0.76 is far from the ratio obtained empirically for the Japanese interplate earthquakes of 0.35 (Tajima et al., 2013).

7. Acknowledgements

I would like to express my sincere appreciation for all technical assistance and sharing to the authorities and researches of CISMID, specially to Carlos Zavala, Zenon Aguilar, Fernando Lazares, and also to Dr. Hernando Tavera, director of the Department of Seismology at the Geophysical Institute of Peru.

8. Copyrights

9. References

References [1, 2], numbered according to the order in which they appear in the text.

[1] Somerville, P., Irikura, K., Graves, R., Sawada, S., Wald, D., Abrahamson, N., Iwasaki, Y., Kagawa, T., Smith, N. and Kowada, A., 1999, Seism. Res. Lett., 70 No. 1, 59-80.

[2] Sladen, A., Tavera, H., Simons, M., Avouac, J. P., Konca, A. O., Perfettini, H., Audin, L., Fielding, E. J., Ortega, F. and Cavagnoud, R., 2010, J. Geophys. Res., Solid Earth, 115, Issue B02405.

[3] Perfettini, H., Avouac, J., Tavera, H., Kositsky, A., Nocquet, J., Bondoux, F., Chlieh, M., Sladen, A., Audin, L., Faber, D., Soler, P., 2010, Nature, 465,

[4] Lay, T., Ammon, Ch., Hutko, A. and Kanamori, H., 2010, Bull. Seis. Soc. Am., 100, 3, 969-994.

[5] Pulido N., Tavera H., Aguilar Z., Nakai S. and Yamazaki F., 2013, J. Disaster Res., Vol 8 N°2.

[6] Irikura, K., 1986, Proceedings of the 7th Japan Earthquake Engineering Symposium, Tokyo, 151-156.

[7] Kanamori, H. and Anderson, D.L., 1975, J. Geophys. Res., 80, Issue 8, 1075-1078.

[8] Aki, K, 1967, J. Geophys. Res., 72, Issue 4, 1217-1231, doi: 10.1029/JZ072i004p01217.

[9] Brune, J. N., 1970, J. Geophys. Res., 75, Issue 26, 4997-5009, doi:10.1029/JB075i026p04997.

[10] Brune, J. N., 1971, Correction, J. Geophys. Res., 75, 4997-5009.

[11] Irikura, K. and Miyake, H., 2015, IISEE Lecture Note 2014-2015, Building Research Institute.

[12] Miyake, H., Iwata, T. and Irikura, K., 2003, Bull. Seis. Soc. Am., 93, 2531-2545.

[13] Sladen, A., 2013, http://www.tectonics.caltech.edu/slip_history/2007_peru/pisco-update.html

[14] Quispe, S., Yamanaka, H., Aguilar, Z., Lazares, F., Tavera, H., 2013, J. of Disaster Research, 8, 2, 243-251.

[15] Velenzuela Bize, J.G., 1997, Individual Studies, IISEE, 33, 181-191.

[16] Murotani, S., Miyake, H. and Koketsu, K., 2008, Earth Planet Space, 60, 987-991.

[17] Tajima, R., Matsumoto, Y., Si, H. and Irikura, K., 2013, Zisin, 66 (In Japanese with English abstract).

[18] Web site: IRIS Data Services: http://ds.iris. edu/spud/backprojection, 2007.

[19] Web site: GEBCO, http://www.gebco.net/